Hindawi
Advances in Materials Science and Engineering
Volume 2023, Article ID 9808135, 1 page
https://doi.org/10.1155/2023/9808135

Retraction

Retracted: Tribological Behavior of AA7075 Reinforced with Ag and ZrO_2 Composites

Advances in Materials Science and Engineering

Received 26 December 2023; Accepted 26 December 2023; Published 29 December 2023

This article has been retracted by Hindawi, as publisher, following an investigation undertaken by the publisher [1]. This investigation has uncovered evidence of systematic manipulation of the publication and peer-review process. We cannot, therefore, vouch for the reliability or integrity of this article.

Please note that this notice is intended solely to alert readers that the peer-review process of this article has been compromised.

Wiley and Hindawi regret that the usual quality checks did not identify these issues before publication and have since put additional measures in place to safeguard research integrity.

We wish to credit our Research Integrity and Research Publishing teams and anonymous and named external researchers and research integrity experts for contributing to this investigation.

The corresponding author, as the representative of all authors, has been given the opportunity to register their agreement or disagreement to this retraction. We have kept a record of any response received.

References

[1] C. R. Mahesha, S. R, M. M. Sree Jayan et al., "Tribological Behavior of AA7075 Reinforced with Ag and ZrO_2 Composites," *Advances in Materials Science and Engineering*, vol. 2022, Article ID 7105770, 8 pages, 2022.

Hindawi
Advances in Materials Science and Engineering
Volume 2022, Article ID 7105770, 8 pages
https://doi.org/10.1155/2022/7105770

Research Article

Tribological Behavior of AA7075 Reinforced with Ag and ZrO_2 Composites

C. R. Mahesha,[1] Suprabha R,[1] M. Mahaveer Sree Jayan,[2] Shilpa Kulkarni,[3] Aman Sharma,[4] Essam A. Al-Ammar,[5] S. M. A. K. Mohammed,[6] Ram Subbiah,[7] and Agonafir Alemayehu[8]

[1]*Department of Industrial Engineering & Management, Dr. Ambedkar Institute of Technology, Bangalore 560056, Karnataka, India*
[2]*Department of Mathematics, Indra Ganesan College of Engineering, Tiruchirapalli 620012, Tamil Nadu, India*
[3]*Department of Physics, Shri Ramdeobaba College of Engineering and Management, Nagpur 440013, Maharashtra, India*
[4]*Department of Mechanical Engineering, GLA University, Mathura, UP 281406, India*
[5]*Department of Electrical Engineering, College of Engineering, King Saud University, 800 Riyadh 11421, Saudi Arabia*
[6]*Department of Mechanical and Industrial Engineering, Ryerson University, Toronto M5B 2K3, ON, Canada*
[7]*Department of Mechanical Engineering, Gokaraju Rangaraju Institute of Engineering and Technology, Hyderabad, Telangana 500090, India*
[8]*Department of Mechanical Engineering, Mizan Tepi University, Mizan Teferi, Ethiopia*

Correspondence should be addressed to Agonafir Alemayehu; agonafir@mtu.edu.et

Received 5 July 2022; Revised 25 August 2022; Accepted 31 August 2022; Published 23 September 2022

Academic Editor: K. Raja

In this study, an AA7075 composite material with a varying weight percentage of silver and zirconium oxide reinforcement is examined in terms of its properties. Reinforcement quantities ranging from 0, 4, 8, 12, and 16 wt % were combined with the matrix using the in-situ technique of stir casting in the field. Tensile, mechanical hardness, and compressive strength were assessed in accordance with the standard. The X-ray diffraction and EDS were utilized to analyze AA7075 composites for the distribution and dispersion of particles. Different input parameters such as load (N), composites (wt %), and velocity (m/s) were used to evaluate wear resistance when using the pin-on-disc method. The wear rate (mm/m) was estimated for every weight percent of reinforced mass loss (g). Optimization methods such as Taguchi and analysis of variance were used to determine the AA7075's optimal processing parameters and composites that were the most significant. In order to identify the best genetic algorithm results, theoretical and experimental results were evaluated.

1. Introduction

Aluminum metal matrix composites play a significant part in today's industrial environment because of their characteristics, weight, and strength ratio [1, 2]. As a result of Al's low density, malleability, better thermal conductivity, and abrasive resistance, it is the second most often employed material in the industry [2–4]. Ceramic reinforcement particles, such as zirconium oxide, Ag, silicon nitride, titanium diboride, TiN, boron carbide, TiC, titanium dioxide, and silicon dioxide, are utilized to make AMCs more potent and effective [5, 6]. These qualities can be improved by manufacturing AMCs using a variety of processes, including squeeze and stir casting, FSW, and PM [7]. AMCs' mechanical qualities are mostly determined by their manufacturing processes. Reinforcement particles' distribution in the matrix material is by far the most important factor here [8]. It is possible to manufacture composite materials using either a solid-state approach or a liquid-state method. The solid-state approach is the more expensive of the two options, thus it is not suggested for large-scale production [9–11]. To put it another way, the liquid-state method has a lower production cost than the solid-state method and is very practicable and assures a proper

distribution of strengthening in the matrix material [12, 13]. Stir casting has been proven to be a simple and economical approach for the in-situ reaction of AMCs [14]. The physical qualities of AA7075 are better than those of other aluminum matrix composites [15]. It was decided to use silver (Ag) as the strengthening material because of its high thermal expansion coefficient, reasonable thermal stabilization, higher strength, and great dispersal properties with Al composites [16]. Due to its electrical and thermal stability, high thermal stability, and superior erosion and corrosion resistance, zirconium oxide is frequently used as a reinforcing ceramic [17]. For the most part, the tribological examinations are conducted by using POD test equipment. AMCs are primarily controlled by the rate of wear and the coefficient of friction [18–21]. Discs of steel or cast iron are used to generate friction on the specimen [22]. Composite tribological behavior processing characteristics are studied and analyzed using DOE. With the least amount of error, Taguchi and ANOVA methodologies are utilized to determine the influence of process characteristics and how much each processing parameter contributes to the overall process percentage [23, 24]. To predict accurately and discover the optimal and average values of output parameters, a genetic algorithm is utilized [25].

As a result of this inquiry, Al7075 composites have been created utilizing various weight percentages (wt %) of reinforcement, such as 0, 4, 8, 12, and 16 Ag and ZrO_2 These composites have been tested for their mechanical properties using hardness, tensile, and compression tests, and by using varying percentages of AA7075. Pin-on-disc wear tests have been conducted with a variety of input parameters. For AA7075 compounds, Taguchi, ANOVA, and GA optimization approaches were utilized to estimate the percentage of every parameter and optimum values.

2. Methods and Materials

2.1. Specimen Fabrication. In this study, the matrix material is AA7075 which is the toughest and heaviest consumer alloy used in multiple parts of the moving sectors and the reinforcement is silver and zirconium oxide particles. In AA7075, by adopting a stir casting process, the composites were created. AA7075 was melted at a temperature of 720°C in a heated furnace. Table 1 lists the composition of AA7075. The melted AA7075 was stirred in with the reinforcing particles before being added. Two powders, KBF_4 and K_2ZrF_6, were used to make zirconium oxide. There were 0, 4, 8, 12, and 16% reinforcing weight percentages in the process [26]. Reinforcing particles silver and zirconium oxide were mixed with the AA7075 matrix at a rate of <15% to ensure strong attachment and equitable spreading in the matrix [27]. According to the hypothesis, the matrix material has avoided one-point segregation due to reinforcement mixing. A 10 mm diameter and 20 mm-long pin mold had already been developed at that point for the new product. Matrix and reinforcements were meticulously combined and put into the mold cavity, which was then allowed to cool before being removed from the container.

2.2. Mechanical Properties. ASTM standards were utilized to evaluate the mechanical characteristics of AA7075 compounds at changing weight percentages in the tests. There is a method for measuring the hardness of composites based on ASTM E10-07 and it is called the Micro Vickers' Hardness testing machine. The indentation was made on each sample in a different location on the five samples that were used in this test. The hardness of the material was measured and an indentation was found in the right area of the reinforcing particles after the measurements were taken. ASTM E08-8 and E09-9 standards were used to determine the tensile [28] and compression strengths, respectively, by employing a universal testing apparatus [29]. Each weight percentage of AA7075 composites was used in the preparation of the samples. In order to eliminate scratches, samples were cleaned with a SiC 1200 grid paper. The tensile test was performed with a weight of 10 KN and a crosshead speed of 2.5 m/min. By deforming samples of AA7075 with different reinforcing weight percentages, compression test forces were computed.

2.3. Wear Test. The wear test was carried out with a pin-on-disc testing instrument. The ATM G99 G95a standard was used throughout the test at room temperature. This study used a total of 25 samples for analysis. The samples had a diameter of 10 mm and a length of 25 mm for the test. An electronic weighing scale was employed to measure the mass loss of the specimen earlier and later they were worn [30]. Abrasive disc friction resulted in mass loss during sample preparation. The input parameters would be the weight percentage of the composites, the load, and the velocity (m/s). Table 2 lists the relevant input parameters. The sliding distance remained constant at 3000 m.

2.4. Optimization Techniques. Taguchi and ANOVA are employed as the optimization approaches of this study because Taguchi is a simple, powerful, and cost-effective approach [31, 32]. The signal-to-noise ratio is typically examined in terms of "smaller is better," "nominal is better," and "bigger is better," among others. In order to attain the lowest wear rate, the criterion "smaller is better" was used in this study. These input parameters are likewise affected by the situation. The L_{25} orthogonal array is shown in Table 3 . MATLAB software is used to implement. Here, the ANOVA approach is utilized to find the most important input factors for the numerical optimization procedure. This program is used to create the design matrix and to identify which composite process factors have the greatest impact on performance [33]. The effects of influencing constraints on the wear rate of AA7075 composites with varying reinforcing levels are summarized in an ANOVA table. The median values of the variables are determined through the use of an ANOVA.

Table 1: Chemical composition of AA7075.

Basics	Silicon	Iron	Copper	Manganese	Magnesium	Chromium	Zinc	Aluminum
Weight percentage	0.05	0.10	1.60	0.05	2.70	0.19	5.80	Remaining

Table 2: Pin-on-disc wears testing input factors.

Input factors	Values
Composites (wt %)	0, 4, 8, 12, and 16
Load (*N*)	15, 25, 35, 45, and 55
Velocity (m/s)	2, 4, 6, 8, and 10

Table 3: L_{25} orthogonal array.

S.No	Composites (wt %)	Load (*N*)	Velocity (m/s)
1	0	15	2
2	0	25	4
3	0	35	6
4	0	45	8
5	0	55	10
6	4	15	4
7	4	25	6
8	4	35	8
9	4	45	10
10	4	55	2
11	8	15	4
12	8	25	6
13	8	35	10
14	8	45	2
15	8	55	8
16	12	15	6
17	12	25	10
18	12	35	2
19	12	45	4
20	12	55	8
21	16	15	10
22	16	25	2
23	16	35	4
24	16	45	8
25	16	55	6

3. Results and Discussion

3.1. Study of Mechanical Characteristics

3.1.1. Study of Hardness Test. Following the in-situ procedure, the microhardness examination was performed with a continuous 0.5 kg load on AA7075 with varying weight percentages of silver and zirconium oxide. In Figure 1, the results of the hardness tests are shown for a variety of reinforcing quantities. The in-situ bonding of the grains increases resistance to the external load only an indentation with the addition of reinforcements with the matrix. It shows that the grain has been refined. In comparison to unreinforced AA7075, the composite surfaces showed no signs of indentation defects. The Orowan reinforcing method assumed that the strengthening particles were evenly dispersed throughout the composites in order to maximize strength. The uniform distribution of particles prevented particle

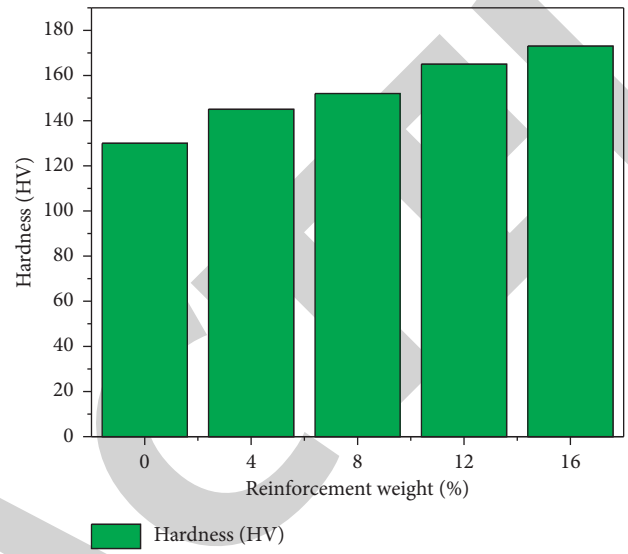

Figure 1: Hardness.

mobility and dislocation. Due to the Orowan loops, dislocation processes were impeded around the reinforcements [34], and because of departure strengthening, the fine interfacial connection and good interface of the AA7075 matrix were achieved. The addition of reinforcing particles gradually increases the AA7075 composite's hardness.

3.1.2. Study of Tensile Strength and Compressive Strength. The tensile strength of composites with different strengthening levels, such as 0, 4, 8, 12, and 16, can be evaluated by use of the universal testing machine (UTM). The matrix evenly distributes the load to the reinforcement particles in each sample, which are prepared to the desired dimensions. The strength of the composites will increase as a result of the homogeneous dispersion and strong connection between the grains [35]. Rendering to the Orowan strengthening process, displacements are constrained and particle arrests take on a bow-shaped structure. Grain dislocation is prevented by the bow-shaped arrest. The bonding becomes extremely high if the dislocations are stopped. As a result, raising the reinforcing weight percentage of composites improves the overall system strength. Continuous gliding results from dislocations that occur outside of the grains throughout time. As can be seen in Figure 2, the tensile test results are obtained.

According to the findings of the tests, the reinforcements steadily enhance the compression strength. Figure 3 shows the test findings in a visual format. For the matrix and reinforcement to be as near together as possible, the in-situ formation is used. Crushing loads are evenly distributed throughout the reinforcements if the ceramic particles are well dispersed. A few little cracks have appeared. Evenly distributed

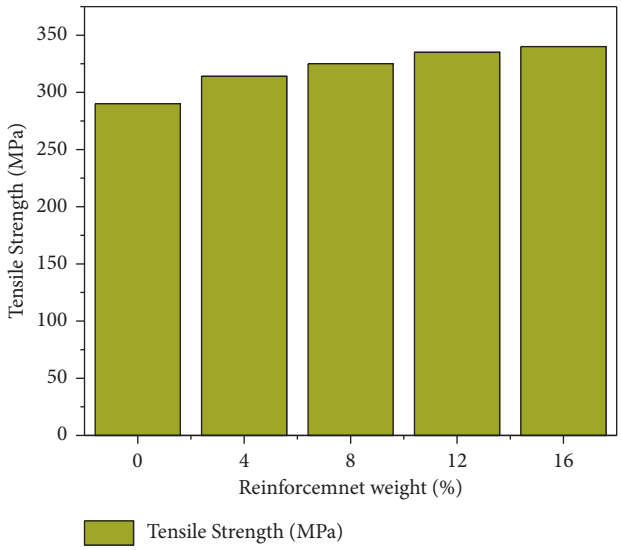

Figure 2: Tensile strength.

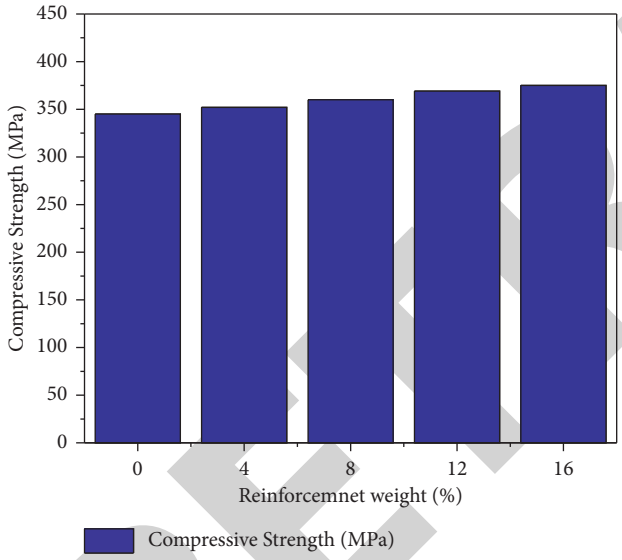

Figure 3: Compression strength.

stresses cause grains to be slightly displaced. As a result, the composites have a modest flexibility to prevent them from breaking apart. External loads are transferred and distributed uniformly through reinforcing particles to the composite material when they are applied. That means that the AA7075 composites with a greater wt percentage (16%) have a better particle distribution and better bonding. As a result, raising the reinforcing weight percentage improves mechanical qualities.

3.2. XRD Evaluation. The analysis of in-situ AA7075 composites shows that different peaks are present in the AA7075 composites with varying reinforcements in the weight percentage range as shown in Figure 4. It is confirmed by XRD that the matrix material contains reinforcements. With the AA7075 matrix, the presence of both

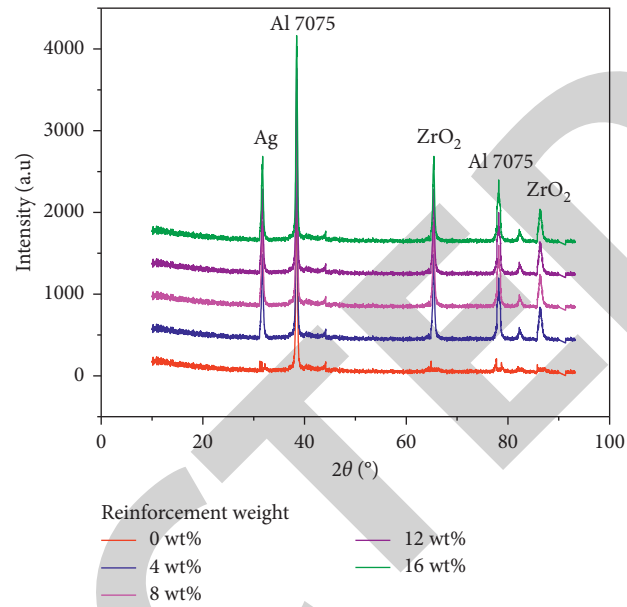

Figure 4: XRD evaluation of AA7075 composites.

reinforcements can be clearly seen. Reinforcements help to boost the intensity of the various peaks of intensity. Aluminum oxide and other metallic compounds can be seen in some of the minor peaks from this reaction. Oxide can be linked with the aluminum matrix during the sintering process, resulting in a green compact. Nitrides and aluminum are combined in a ratio that is less than or equal to. There is an increase in the zirconium oxide mass fraction signal strength, indicating that mass fraction limitations are conceivable. These chemicals, however, were not detected by XRD.

3.3. EDS Analysis. The analysis of the AA7075 composites with different reinforcing levels is shown in Figure 5. It is a quantitative and qualitative examination of the 7075 matrix component constituents found in an aluminum alloy. The mixing of matrix and reinforcements was confirmed by the EDS spectrograph. The largest peak of aluminum was detected during EDS analysis following the wear test. Wearing surfaces may develop some oxidation over time owing to exposure to heat. The apex of the reinforcement was also identified. In the process of mechanical alloying, iron is transferred from the wear surface to the reinforcements. In order to withstand the atomic changes caused by wear, the iron layer is thickened to boost resistance. An aluminum-nitride association is visible on the spectrograph during wear.

4. Experimentation on Optimization Results

4.1. Taguchi Optimizing Methodology. The optimization of metal matrix details was achieved by using L_{25} orthogonal arrays in this study (OA). The manufacturing and machine mistakes were perfected after approximately 25 experiments with various input constraints were conducted. The majority of the material, AA7075, was blended with other impurities in

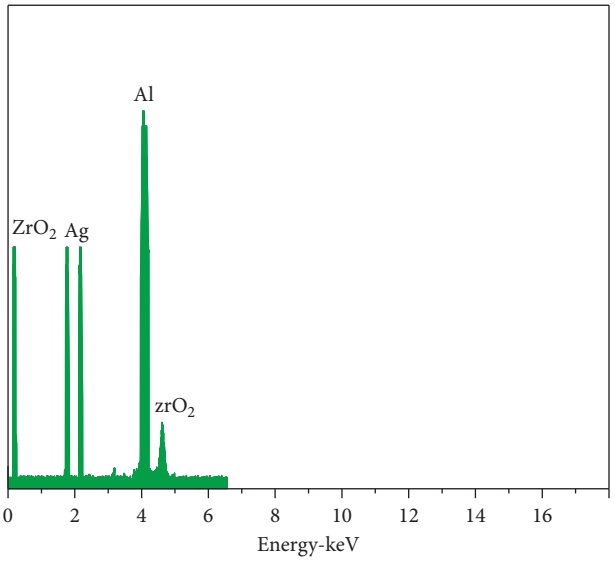

Figure 5: EDS analysis.

order to improve the results by considering three different elements, including the composite weight percentage, velocity, and load. It was decided to keep the wear rate as the primary responsive factor. Overall, there were 25 experiments, each of which had five runs for each processing factor. Costs for wear and tear were typically low. Using the repeated formula $-10 \times \text{Log10}\ (\text{sum}\ (Y^2)/n)$, the results of these 25 experiments were combined. Observations have shown that increasing the weight percentage resulted in a decrease in the wear rate. By using the pin-on-disc apparatus, the pin exerted 20 N of force on the disc and the disc travelled at 1 m/s, the POD device recorded a minimal wear rate of 0.000182 mm^3/m. Results that are closer to the ideal are shown in Table 4.

4.2. S/N Ratio. The DOE provides the body size to figure out the authority variables in order to reduce the procedure by lowering the noise. The reduction of these variables is accomplished through iterative processes including some delta values. Depending on the situation, the *S*/*N* ratio will have different data characteristics. It is necessary to utilize "nonnegative with a target value of zero" when calculating the rate at which an object is wearing out. This group will have the lowest response rate and the best outcome. Data mean repetition values and the signal-to-noise ratio are presented in Tables 5 and 6. In both circumstances, the composite weight percentage increases the MMC strength and reduces the wear rate to a minimum. Figure 6 provides graphic charts of the wear rate. Abrasion rate *Y* axis has been used to analyze the graph by maintaining the data mean value constant.

4.3. ANOVA. Analysis of Variance is an arithmetical examination of the difference between groups that establishes ideal divisions between the aspects of the data. The statistical test comparing mean values is utilized to determine the influence of procedure elements that yield better outcomes. Each individual parameter's percentage of

Table 4: Experimental runs input and output values.

S. No	Composites (wt %)	Load (*N*)	Velocity (m/s)	Wear rate (mm^3/m)
1	0	15	2	0.005140
2	0	25	4	0.006630
3	0	35	6	0.005720
4	0	45	8	0.005620
5	0	55	10	0.000820
6	4	15	4	0.004270
7	4	25	6	0.003805
8	4	35	8	0.006409
9	4	45	10	0.003408
10	4	55	2	0.002607
11	8	15	4	0.000796
12	8	25	6	0.001865
13	8	35	10	0.001816
14	8	45	2	0.002586
15	8	55	8	0.001907
16	12	15	6	0.001589
17	12	25	10	0.001589
18	12	35	2	0.001639
19	12	45	4	0.001249
20	12	55	8	0.001199
21	16	15	10	0.000885
22	16	25	2	0.000182
23	16	35	4	0.000586
24	16	45	8	0.000787
25	16	55	6	0.000885

Table 5: *S*/*N* ratio's response.

Level	Composites	Load	Velocity
1	45.42	55.72	57.42
2	49.34	56.76	54.73
3	56.72	53.95	56.34
4	58.23	54.62	53.35
5	65.84	54.67	53.78
Delta	21.53	3.81	4.26
Rank	1	3	2

Table 6: Means response.

Level	Composites	Load	Velocity
1	0.006152	0.002548	0.002407
2	0.005063	0.002872	0.002903
3	0.001872	0.003293	0.002538
4	0.001492	0.002788	0.004354
5	0.000673	0.002936	0.004126
Delta	0.006479	0.000853	0.000962
Rank	1	3	2

inheritance is listed in Table 7. A visual representation of the inheritance percentage is shown in Figure 7. With the percentage of process variables that can be inherited, it can be stated that the weight percentage of AA7075 helps lift the wear resistance of the matrices with other impurities. Nearly, 81% of the contributions came from the weight percentage of the population. The remainder of the proportion is made up of the other two variables, velocity (8%) and load (15%). Experimental and statistical analyses are

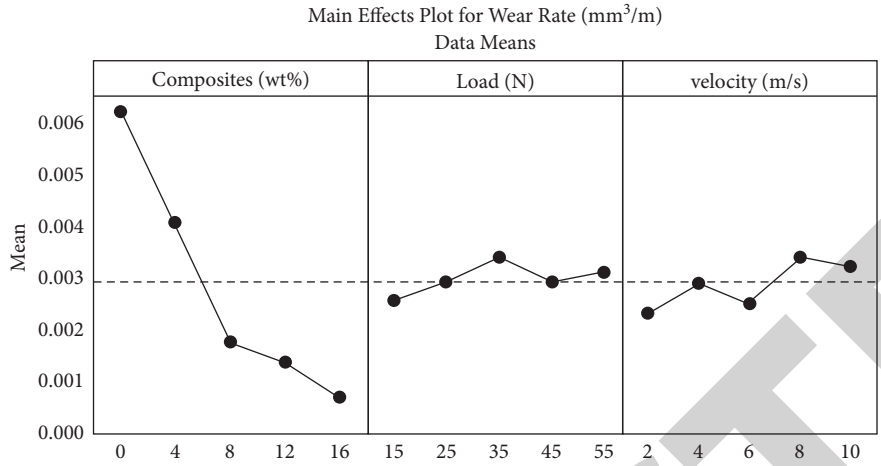

Figure 6: Main effect plot for the wear rate.

Table 7: ANOVA wear rate.

Source	DF	Adj.SS	Adj.MS	*F* value	*P* value	% of contribution
Composites (wt %)	4	0.000101	0.000026	25.63	0	87
Load (*N*)	4	0.000003	0	0.39	0.817	3
Velocity (m/s)	4	0.000011	0.000002	0.88	0.508	10
Error	12	0.000003	0.000002			0
Total	24	0.000118				100

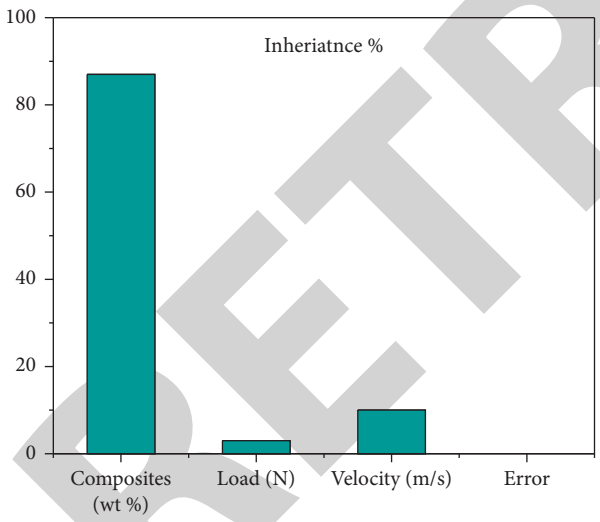

Figure 7: Inheritance % of processing parameters.

Table 8: Comparison of Taguchi and experimental techniques.

Techniques	*Input factors*			*Output factors*
Units	Composites (wt %)	Load (*N*)	Velocity (m/s)	Wear rate (mm^3/m)
Taguchi	16	25	2	0.000182
Experimental	16	25	2	0.0003

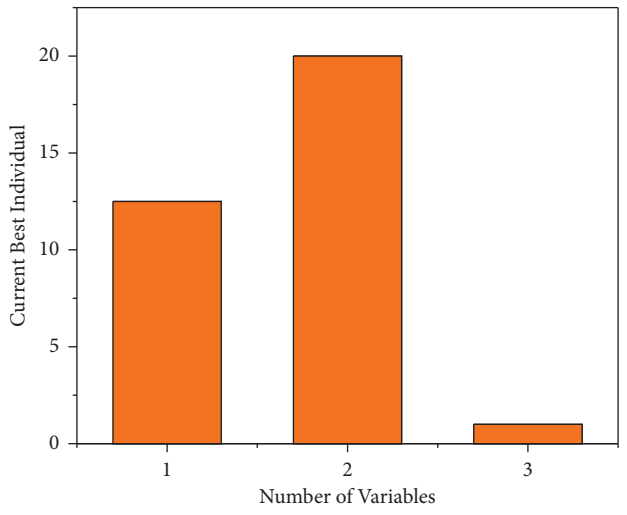

Figure 8: Minimal wear rate estimation output attained by the GA.

contrasted in Table 8, which clarify the comparative assertions. Slight differences between the two methods are spread over the world. Accordingly, it can be concluded that the research strategy is a success since the input variables of 16 wt % of the compound, 25 N and 2 m/s segregate superior abrasive resistance better than earlier cycle runs of the experiment.

4.4. Wear Rate by Genetic Algorithm. After the MATLAB code was fitted to train the software, a nontraditional technique was used to forecast input and output variables to infinity uniformly. GA mimics the natural screening, in which the fittest individuals are chosen for procreation to produce the following generation. It was possible to obtain

Table 9: Comparison of genetic algorithms and experimental techniques.

Techniques	*Input factors*			*Output factors*
Units	Composites (wt %)	Load (N)	Velocity (m/s)	Wear rate (mm^3/m)
Genetic algorithm	16	25	2	0.000162
Experimental values	16	25	2	0.000182

the fitness function from a variety of mathematical models. According to the variables depicted in Figure 8, we were able to maximize the findings. According to the findings, the lowest wear rate was reached by using 16 wt% composite, 25 N, and 2 m/s to achieve 0.000182 MPa, while the data average value has changed equal to 0.000262 MPa. Tables 8 and 9 show the comparison between the actual experimental value and the software's prediction. When the projected values of process parameters differ somewhat from what is actually observed in the laboratory, then the GA can maintain its high standards.

5. Conclusion

Through the in-situ creation of AA7075 composites, the stir casting method was well created with varying amounts of reinforcements with 0, 4, 8, 12, and 16 wt %.

(i) Mechanical properties of AA7075 composites ensured that no particles were dislocated in the composites and that the load was uniformly dispersed among the strengthening. Mechanical qualities improved as reinforcements were added. Parameters were shuffled using the L_{25} orthogonal array. The higher the percentage of reinforcement, the lower was the wear rate. Taguchi and investigational data show that reinforced composites at 16 wt% have a lower wear rate of 0.000182 mm^3/m, whereas experimental value is 0.0003 mm^3/m.

(ii) The grain refinement procedure was successful and faults were evaded because of the firm link between the matrix and the strengthened particles. An investigation of the XRD and EDS data exposed the conformation of the AA7075 composites fillers and ingredients, respectively.

(iii) In this study, the best and average wear rates were found. The GA and experimental comparisons were extremely close.

Data Availability

The data supporting the current study are given in the article and further information or data are available from the corresponding author on reasonable request.

Conflicts of Interest

The authors declare that they have no conflicts of interest.

Acknowledgments

The authors would like to thank MizanTepi University, Ethiopia, for their support and help during the research and for preparation of the manuscript. This work was funded by the Researchers Supporting Project Number (RSP2022R492), King Saud University, Riyadh, Saudi Arabia.

References

[1] D. Kumar, S. Angra, and S. Singh, "Mechanical properties and wear behaviour of stir cast aluminum metal matrix composite: a review," *International Journal of Engineering*, vol. 35, no. 04, pp. 794–801, 2022.

[2] S. Bezzina, E. B. Moustafa, and M. A. Taha, "Effects of metastable θ' precipitates on the strengthening, wear and electrical behaviors of Al 2519-SiC/fly ash hybrid nanocomposites synthesized by powder metallurgy technique," *Silicon*, 2022.

[3] O. O. Edosa, F. K. Tekweme, and K. Gupta, "A review on the influence of process parameters on powder metallurgy parts," *Eng. Appl. Sci. Res*, vol. 49, no. 3, pp. 433–443, 2022.

[4] T. Sathish, S. D. Kumar, M. Ravichandran, V. Mohanavel, S. S. Kumar, and S. Rajkumar, "Lead-free piezoelectric ceramics of (Bi1/2Na1/2)TiO3- system," *Key Engineering Materials*, vol. 928, pp. 69–78, 2022.

[5] S. Pan, K. Jin, T. Wang, Z. Zhang, L. Zheng, and N. Umehara, "Metal matrix nanocomposites in tribology: manufacturing, performance, and mechanisms," *Friction*, vol. 7, 2022.

[6] K. Subramani, T. Arunkumar, V. Mohanavel et al., "Investigation on wear characteristics of Al 2219/Si3N4/Coal bottom ash MMC," *Materials Today Proceedings*, vol. 62, no. 8, pp. 5514–5518, 2022.

[7] M. Ravichandran and M. Ravichandran, "Influence of AlN particles on microstructure, mechanical and tribological behaviour in AA6351 aluminum alloy," *Materials Research Express*, vol. 6, no. 10, Article ID 106557, 2019.

[8] M. Honarpisheh and M. Honarpisheh, "Experimental and numerical investigation of process parameters on the residual stresses in the Al-Cu FGM materials," *Experimental Techniques*, vol. 45, no. 5, pp. 601–612, 2021.

[9] A. Fattah-alhosseini, R. Chaharmahali, M. K. Keshavarz, and K. Babaei, "Surface characterization of bioceramic coatings on Zr and its alloys using plasma electrolytic oxidation (PEO): a review," *Surfaces and Interfaces*, vol. 25, Article ID 101283, 2021.

[10] D. Srinivasan, M. Meignanamoorthy, A. Gacem et al., "Tribological behavior of Al/Nanomagnesium/Aluminum nitride composite synthesized through liquid metallurgy technique," *Journal of Nanomaterials*, vol. 2022, Article ID 7840939, 12 pages, 2022.

[11] L. Kang, W. Liu, X. Zhang, and L. Chen, "Evolution of microstructure, texture and residual stress of AZ31 Mg alloy in hot extrusion process," *Materials Research Express*, vol. 8, no. 6, Article ID 066519, 2021.

[12] I. S. Patil, S. S. Rao, and M. A. Herbert, "Mechanical and microstructural analysis of a AlSi-ZrO2 metal matrix composite using optimized artificial neural network and experimental data," *Materials Today Communications*, vol. 27, Article ID 102398, 2021.

[13] O. Güler, T. Varol, Ü. Alver, G. Kaya, and F. Yıldız, "Microstructure and wear characterization of Al2O3 reinforced silver coated copper matrix composites by electroless plating

and hot pressing methods," *Materials Today Communications*, vol. 27, Article ID 102205, 2021.

[14] N. A. Costa, A. L. Rossi, A. C. Alves, A. M. P. Pinto, F. Toptan, and L. A. Rocha, "Growth mechanisms and tribocorrosion behavior of bio-functionalized ZrO2 nanoparticles-containing MAO coatings formed on Ti-40Nb alloy," *Journal of Bio- and Tribo-Corrosion*, vol. 7, no. 2, p. 53, 2021.

[15] M. Elmahdy and M. Elmahdy, "Study of mechanical properties and wear resistance of nanostructured Al 1100/TiO2 nanocomposite processed by accumulative roll bonding," *Journal of Composite Materials*, vol. 56, no. 17, pp. 2727–2738, 2022.

[16] M. Molaei, A. Fattah-alhosseini, M. Nouri, P. Mahmoodi, S. H. Navard, and A. Nourian, "Enhancing cytocompatibility, antibacterial activity and corrosion resistance of PEO coatings on titanium using incorporated ZrO2 nanoparticles," *Surfaces and Interfaces*, vol. 30, Article ID 101967, 2022.

[17] P. Li, "Investigation of biodegradability, cytocompatibility and antibacterial property of plasma electrolytic oxidation coating on Mg," *surface and interface*, vol. 30, Article ID 101840, 2022.

[18] A. Mazur-Nowacka, "Influence of Zirconia and Organic Additives on Mechanical and Electrochemical Properties of Silica Sol-Gel Coatings," *Materials*, vol. 14, no. 9, p. 2389, 2021.

[19] Z. Leman, "AA7075-ZrO2 Nanocomposites Produced by the Consecutive Solid-State Process: A Review of Characterisation and Potential Applications," *Metals*, vol. 11, no. 5, p. 805, 2021.

[20] T. Varol, O. Güler, S. B. Akçay, and H. C. Aksa, "The effect of silver coated copper particle content on the properties of novel Cu-Ag alloys prepared by hot pressing method," *Powder Technology*, vol. 384, pp. 236–246, 2021.

[21] M. Kaseem, S. Fatimah, N. Nashrah, and Y. G. Ko, "Recent progress in surface modification of metals coated by plasma electrolytic oxidation: principle, structure, and performance," *Progress in Materials Science*, vol. 117, Article ID 100735, 2021.

[22] R. K. Nayak, M. K. Pradhan, and A. K. Sahoo, *Machining of Nanocomposites*, CRC Press, Boca Raton, Florida, 2022.

[23] S. Balaji, P. Maniarasan, S. V. Alagarsamy et al., "Optimization and Prediction of Tribological Behaviour of Al-Fe-Si Alloy-Based Nanograin-Refined Composites Using Taguchi with Response Surface Methodology," *Green Nanometal Oxides for Environmental and Biomedical Applications*, pp. 1–12, Article ID 9733264, 2022.

[24] M. S. Abd-Elwahed, A. M. Sadoun, and M. Elmahdy, "Electroless-plating of Ag nanoparticles on Al2O3 for enhanced mechanical and wear properties of Cu-Al2O3 nanocomposites," *Journal of Materials Research and Technology*, vol. 9, no. 6, pp. 13749–13758, 2020.

[25] A. M. Sadoun, I. R. Najjar, G. S. Alsoruji, M. S. Abd-Elwahed, M. A. Elaziz, and A. Fathy, "Utilization of improved machine learning method based on artificial hummingbird algorithm to predict the tribological behavior of Cu-Al2O3 nanocomposites synthesized by in situ method," *Mathematics*, vol. 10, no. 8, pp. 1266–8, 2022.

[26] J. James, A. R. Annamalai, A. Muthuchamy, and C.-P. Jen, "Effect of wettability and uniform distribution of reinforcement particle on mechanical property (tensile) in aluminum metal matrix composite-A review," *Nanomaterials*, vol. 11, no. 9, p. 2230, 2021.

[27] O. Güler, T. Varol, Ü. Alver, and A. Canakci, "Effect of Al2O3 content and milling time on the properties of silver coated Cu matrix composites fabricated by electroless plating and hot pressing," *Materials Today Communications*, vol. 24, Article ID 101153, 2020.

[28] D.-C. Chen, Ci-S. You, and Fu-Y. Gao, "Analysis and experiment of 7075 aluminum alloy tensile test," *Procedia Engineering*, vol. 81, pp. 1252–1258, 2014.

[29] W. S. Hassanein, A. M. Sadoun, and A. Abu-Oqail, "Effect of SiC addition on the mechanical properties and wear behavior of Al-SiC nanocomposites produced by accumulative roll bonding," *Materials Research Express*, vol. 7, no. 7, Article ID 075006, 2020.

[30] A. Sadoun, A. Ibrahim, and A. W. Abdallah, "Fabrication and evaluation of tribological properties of Al2O3 coated Ag reinforced copper matrix nanocomposite by mechanical alloying," *Journal of Asian Ceramic Societies*, vol. 8, no. 4, pp. 1228–1238, 2020.

[31] A. Ibrahim and A. Ibrahim, "WITHDRAWN: microstructure and tribological properties of alumina coating reinforced copper matrix nanocomposite," *Ceramics International*, 2020.

[32] A. M. Sadoun, M. M. Mohammed, A. Fathy, and O. A. El-Kady, "Effect of Al2O3 addition on hardness and wear behavior of Cu-Al2O3 electro-less coated Ag nanocomposite," *Journal of Materials Research and Technology*, vol. 9, no. 3, pp. 5024–5033, 2020.

[33] V. Mohanavel and M. Ravichandran, "Optimization of parameters to improve the properties of AA7178/Si3N4 composites employing Taguchi approach," *Silicon*, vol. 14, no. 4, pp. 1381–1394, 2022.

[34] S. E. Hernández-Martínez, J. J. Cruz-Rivera, C. G. Garay-Reyes, and J. L. Hernández-Rivera, "Experimental and numerical analyses of the consolidation process of AA 7075–2 wt.% ZrO2 powders by equal channel angular pressing," *Journal of Materials Engineering and Performance*, vol. 28, no. 1, pp. 154–161, 2019.

[35] A. Annamalai and A. R. Annamalai, "Machinability study of developed composite AA6061-ZrO2 and analysis of influence of MQL," *Metals*, vol. 8, no. 7, pp. 472–7, 2018.